Published in final edited form as:
Photochem Photobiol. 2004 ; 80: 1–6. doi:10.1562/2004-03-01-RA-093.1.

Spatial Control of Reactive Oxygen Species Formation in Fibroblasts Using Two-photon Excitation¶

Brett A. King† and **Dennis H. Oh***
Department of Dermatology, University of California, San Francisco, CA Dermatology Research Unit, San Francisco Veterans Affairs Medical Center, San Francisco, CA

Abstract

Two-photon excitation (2PE) provides a means of generating reactive oxygen species (ROS) in cells and tissues with a high degree of spatial specificity. In cultured monolayers of human fibroblasts and fibroblast-derived cells treated with the commonly used probe of ROS formation, 5-(and 6)-chloromethyl-2′,7′-dichlorodihydrofluorescein diacetate, acetyl ester (CM-H_2DCFDA), cells irradiated through a microscope objective with 150 fs near-infrared laser pulses became highly fluorescent, reflecting intracellular ROS formation. The fluorescence intensity inside cells increased quadratically with the average power of radiation for pulsed excitation and was unchanged for continuous wave irradiation with the same average power. Single fibroblasts embedded within dermal equivalents were also targeted in this manner and formed ROS, whereas neighboring unirradiated cells were spared. These results demonstrate that ROS can be generated intracellularly in skin cells using 2PE of the metabolic or oxidative products of CM-H_2DCFDA and that formation of ROS can be localized in both cell monolayers and in a tissue equivalent. This technique should be useful in understanding the response of whole tissues such as skin to local generation of ROS and may have applications in photodynamic therapy.

INTRODUCTION

Reactive oxygen species (ROS) are important mediators of cellular toxicity resulting from oxidative stress. When excited by light, certain chromophores generate ROS that are able to damage cells (1). This phenomenon underlies diseases such as the cutaneous porphyrias and some phototoxic drug reactions in which the skin accumulates chromophores that absorb solar radiation and subsequently generate products that either are cytotoxic or elicit an immune response (2). On the other hand, photodynamic agents such as porphyrins have also been exploited to treat a wide variety of medical and dermatologic conditions, including malignant tumors and inflammatory dermatoses such as psoriasis (1,3). Although photodynamic therapy is primarily toxic to pathogenic cells (3), collateral damage may also occur in normal cells that have incorporated the photodynamic agent and reside in the incident light path. Other limitations are light scattering and absorption by tissue that make deep targets such as dermal tumors less accessible to the visible and ultraviolet wavelengths commonly used in photodynamic and photochemotherapy (4).

¶Posted on the website on 28 May 2004.

*To whom correspondence should be addressed: Dermatology Service (190), San Francisco VA Medical Center, 4150 Clement Street, San Francisco, CA 94121. Fax: 415-751-3927; dennisoh@itsa.ucsf.edu.
†Current address: Yale University School of Medicine, New Haven, CT.

For a variety of purposes, one would like to photodynamically induce damage only in specific cellular targets while sparing other adjacent cells. However, our ability to dissect and understand the biological response to photodynamic damage in whole tissues, much less control it, is currently limited. Conventional experimental approaches must either damage multiple cell types of the many layers of the skin or study damage in relatively homogeneous cultured cells dissociated from their normal tissue milieu and architecture. These methods are particularly disadvantageous in the study of cutaneous biology because the skin is highly ordered both spatially and functionally, with a stratified squamous epithelium or epidermis composed of keratinocytes overlying a connective tissue dermis containing fibroblasts. Localizing photodynamic damage to specific cells or groups of cells in different cell layers of a tissue would therefore be useful to study cell–cell interactions in intact skin and would improve the specificity and therapeutic index of photodynamic therapy.

Two-photon excitation (2PE) has been investigated as a means to excite chromophores and initiate photochemistry with three-dimensional specificity (5–11). 2PE occurs when a molecule simultaneously absorbs two photons whose energies are individually insufficient to cause an electronic transition but whose combined energies correspond to the energy gap between two molecular states (12). Because the selection rules for one- and two-photon transitions differ, it is possible that 2PE can occur at energies where no corresponding one-photon absorption exists (13). Although 2PE probabilities of molecules are very small relative to one-photon absorption probabilities, they are proportional to the square of the intensity of incident light and can become significant with the high fluences achievable with pulsed lasers. Most importantly, this quadratic dependence on light intensity permits a focused laser beam to excite molecules in a spatially restricted manner.

2PE has found applications in three-dimensional microscopic imaging as well as in perturbing biological systems (8,9,14–20). 2PE has been used to generate ROS by organic photosensitizers (10), modify biologically relevant molecules (8,16–18) and induce volume-specific photochemistry, including uncaging reactions within single cells (14) and in neuronal tissue (15). We have previously demonstrated that near-infrared 2PE causes psoralens to form adducts with DNA in both fibroblasts and in a three-dimensional tissue phantom (9). 2PE has also been inferred from biological effects after irradiation with near-infrared femtosecond pulses of isolated cells (19) as well as cells treated with protoporphyrin or aminolevulinic acid (21). Even pulsed 1047 nm laser treatment of melanomas in rats has been reported, though the effects were not clearly related to a multiphoton absorption event because 1047 nm continuous wave irradiation was similarly effective (20). To our knowledge, however, there has not yet been rigorous proof of 2PE of a photodynamic agent to target photodynamic damage in tissues with three-dimensional specificity.

ROS are commonly detected using the fluorogenic probe, 2′,7′-dichlorodihydrofluorescein (H_2DCF) or its derivatives (22–24). This nonfluorescent molecule is oxidized by ROS to form the fluorophore 2′,7′-dichlorofluorescein (DCF). DCF has also recently been shown to be a photosensitizer of ROS formation when irradiated with near-ultraviolet radiation (23). In this work we exploit these properties and demonstrate that cells treated with a derivative of H_2DCF and irradiated with 150 fs 800 nm pulsed titanium–sapphire laser form DCF, indicative of ROS formation due to 2PE. We then use this methodology to target ROS formation to individual cells within both cell monolayers and three-dimensional biomimetic tissues of fibroblasts embedded in a collagen matrix while sparing neighboring cells.

MATERIALS AND METHODS

Cells

Normal human dermal fibroblasts were obtained from foreskin of healthy neonates. Fibroblasts (used within five passages) as well as transformed fibroblast-derived HT1080 and XP12RO-SV40 cells were cultured as monolayers in Dulbecco's modified Eagle medium (DMEM) supplemented with 10% fetal bovine serum as previously described (25,26). Normal fibroblasts were incorporated into collagen lattices to form dermal equivalents as previously described (25). Before experimental treatment and microscopic observation, cells were plated on or dermal equivalents were transferred to chambered #1 borosilicate slides (Nalge Nunc International, Naperville, IL) and then washed and incubated with serum-free DMEM lacking phenol red.

Absorption and fluorescence spectroscopy

Absorption spectra were obtained on a Beckman DU-530 spectrophotometer (Fullerton, CA). Intracellular fluorescence spectra were obtained using an LSM 510 META laser-scanning microscope (Carl Zeiss, Jena, Germany).

Generation and observation of ROS

5-(and 6-)Chloromethyl-2′,7′-dichlorodihydrofluorescein diacetate, acetyl ester (CM-H_2DCFDA, Molecular Probes, Inc., Eugene, OR) is a nonfluorescent probe of ROS that diffuses into cells where thiols may react with the chloromethyl groups and esterases hydrolyze the acetate groups, theoretically enhancing intracellular retention (27). On oxidation by ROS, the probe becomes a derivative of the fluorophore DCF. Therefore, ROS generation is detected by measuring fluorescence from this derivative of DCF, which because of its similarity to DCF is called DCF throughout this article. CM-H_2DCFDA was prepared as a stock solution in ethanol or dimethyl sulfoxide. Monolayers or dermal equivalents were incubated in DMEM with 10 μ*M* CM-H_2DCFDA at 37°C in the dark for 30 min. After incubation with CM-H_2DCFDA, dermal equivalents were immobilized against the bottom of the slide either by placing a coverslip on top of them or by removing a portion of the surrounding media. A LSM 510 META microscope capable of multiphoton excitation using a mode-locked (80 MHz, 150 fs FWHM, 6 nm bandwidth) titanium–sapphire laser (Coherent, Inc., Santa Clara, CA) tuned to 800 nm was used to both photoexicite and image samples. The laser was focused with a 20× objective (NA, 0.75) to give an average power at the sample of 5–20 mW, which yielded good contrast and did not result in detectable morphological changes in irradiated cells indicative of injury during the time of the experiment (30–60 min). The excitation power at each wavelength was measured with a LaserCheck power meter (Coherent, Inc., Auburn, CA) before and after each experiment. Under these conditions, a typical average power of 15 mW used for 2PE corresponded to a peak power density of 3×10^{11} W/cm^2 (28). Several approaches for estimating 2PE volumes within a focused laser beam have been described (8,29,30). Based on one approach, at least 50% of the 2PE effect by 800 nm pulsed radiation would be expected to exist within a 0.4 μm diameter at the focal point and 1.5 μm above and below the focal plane (30), assuming that the absorbing species is homogeneously distributed in three-dimensions. Before 2PE, a transmission image of the cells in the visual field was collected using the 633 nm line (5 μW) of a helium–neon laser. Subcellular regions of cells, single cells and groups of cells within the visual field were specified as targets using a function of the microscope software that allows the user to specify an arbitrary area or region of interest (ROI) within the visual field to be scanned. ROI typically comprised 5000 to 15 000 pixels and were scanned 10–30 times with the 800 nm pulsed output of the titanium–sapphire laser with a dwell time of 25 μs/pixel. Fluorescence from DCF was detected by scanning the visual field once with a 1.97 μs/pixel dwell time with either the 488 nm output of the argon ion laser (50 μW) or the pulsed

800 nm titanium–sapphire laser (5 mW) and by placing a 500–550 nm bandpass filter before the detector. Images were analyzed using LSM 510 META software.

RESULTS

CM-H_2DCFDA is a fluorogenic probe of ROS that diffuses into cells. On oxidation by ROS, the probe becomes a derivative of the fluorophore DCF, and fluorescence at 527 nm indicates the generation of ROS. As shown in Fig. 1, CM-H_2DCFDA in pH 7.4 phosphate-buffered saline has little absorption in the visible and near-ultraviolet regions. Spontaneous hydrolysis of the acetate groups at pH 7.4 and oxidation in the presence of 100 μ*M* H_2O_2 resulted in the appearance of absorption and emission bands at 510 and 527 nm, respectively, characteristic of DCF (23,27). When HT1080 cells were incubated with 10 μ*M* CM-H_2DCFDA and then treated with 100 μ*M* H_2O_2, excitation at 488 nm resulted in bright green fluorescence centered at 527 nm, again characteristic of DCF (23,27).

To generate ROS photochemically within cells, normal human dermal fibroblasts were incubated in the dark with CM-H_2DCFDA and subsequently subjected to a pulsed 800 nm laser (Fig. 2). Irradiated cells displayed strong fluorescence from DCF, indicative of ROS formation. Notably, in a confluent monolayer, fluorescence from target cells was significantly greater than that from adjacent neighbors, indicating that both targeting individual cells with the laser is possible and that the fluorophore does not readily migrate between cells after irradiation. The low levels of fluorescence that occur in unirradiated cells over time likely result from endogenous basal metabolic generation of ROS. In separate control experiments in which cells were first irradiated at 800 nm and then immediately incubated with CM-H_2DCFDA and observed within 2 min, there was no more fluorescence observed in irradiated cells than in unirradiated cells (data not shown). Although this is not proof, this result is consistent with the notion that the ROS observed in Fig. 2 do not result from an endogenous chromophore.

To confirm that the ROS signal was generated by 2PE, HT1080 or XP12RO-SV40 cells were incubated with CM-H_2DCFDA and then irradiated with different intensities of the pulsed 800 nm laser. These cells were chosen for this experiment because they possessed more uniform shapes and dimensions than conventional fibroblasts and proved easier to irradiate with a circular ROI of approximately the same size as the target cell. Pairs of similarly sized cells were chosen to facilitate comparison of fluorescence intensities after irradiation. As shown in Fig. 3a, irradiation of cells of comparable size with 15 mW of pulsed 800 nm laser yielded disproportionately brighter cells than did excitation with 7.5 mW. Multiple pairs of cells were irradiated. One cell of each pair received 1.33- or 2-fold the laser excitation power of the other cell, and the resulting fluorescence from DCF was quantified. Figure 3b demonstrates that increasing the excitation power 1.33-fold resulted in a 2-fold enhancement in fluorescence intensity, whereas increasing the excitation power 2-fold resulted in a 4.3-fold enhancement. These results compare favorably with the predicted values of 1.8 and 4.0 for 2PE, indicating that the fluorescence intensity is quadratically dependent on the incident laser excitation power (Fig. 3b).

To further show that ROS generation is due to two- and not one-photon absorption of light, XP12RO-SV40 cells were irradiated with the 800 nm output of the titanium–sapphire laser either in continuous wave mode or pulsed at 80 MHz (Fig. 4). The average power was the same with both types of excitation. Circular ROI of identical diameter were chosen in either nuclear or cytoplasmic regions, and these defined the areas scanned by the laser (Fig. 4a). Cells irradiated with the pulsed output of the titanium–sapphire laser fluoresced brightly, whereas those irradiated with the laser in continuous wave mode did not have any more signal than nonirradiated cells (Fig. 4b), again indicating that 2PE is required to generate ROS. Excitation

limited to the cytoplasm generated ROS throughout the entire cell, including the nucleus, and *vice versa*, demonstrating that focally generated ROS likely rapidly diffuse throughout the cell.

Fibroblasts embedded in a collagen lattice (dermal equivalent) were used to test the ability of 2PE to target ROS formation to specific cells within a three-dimensional tissue-like environment (Fig. 5). Dermal equivalents were typically 1–3 mm thick and appeared slightly opaque, though translucent. The transmission of 800 nm light through a 1 mm thick dermal equivalent was about 70%. The incident titanium–sapphire laser beam was introduced though the borosilicate glass bottom of the culture chamber before entering the bottom of the dermal equivalent and focusing at a plane inside the dermal equivalent. Figure 5a shows a plane 25 μm within the dermal equivalent after incubation with CM-H_2DCFDA but before irradiation with the pulsed 800 nm titanium–sapphire laser. After 2PE, only the two cells in the center of the 25 μm plane that were exposed to 2PE exhibited increased fluorescence, indicative of ROS generation, whereas surrounding cells in and out of the focal plane remained unchanged (Fig. 5b,d). Irradiation of two additional cells in the 25 μm plane resulted in fluorescence in those cells as well, while continuing to spare neighboring cells in the dermal equivalent (Fig. 5c,e). Notably, some cells seen above and below the target cells in Fig. 5d,e were in the incident laser beam but lay in nonfocal planes and thus did not exhibit fluorescence above background.

DISCUSSION

Multiphoton excitation is now commonly used to image three-dimensional biological materials (21,31,32), and recently work has focused on using this technique to affect chemical changes (8–11,14–19,21,30). However, little work has extended multiphoton excitation to create chemical changes in tissues with three-dimensional precision (14,15). We have previously demonstrated that 2PE is capable of inducing photochemical DNA adduct formation with spatial specificity (9). The focus of this study was to extend 2PE to target ROS formation to individual cells within an intact biomimetic tissue similar to human dermis.

H_2DCF and its derivatives are commonly used to probe for the presence of ROS. When oxidized to DCF by ROS, the probe becomes a fluorophore (27). Previous work by others suggests but has not shown that 2PE of DCF and subsequent induction of ROS is possible. First, Chignell and coworkers have demonstrated that DCF is not only a reporter of ROS but also undergoes complex photochemistry, acting as a photosensitizer of both H_2DCF oxidation and ROS formation on absorption of light (22,24). Second, the parent molecule of DCF, fluorescein, has been shown to have significant 2PE cross-sections between 690–1050 nm (13,28). That fluorescein undergoes 2PE at 800 nm but does not have significant one-photon absorption at 400 nm likely reflects the differing selection rules governing one-photon excitation (1PE) and 2PE. Third, the emission spectrum of fluorescein is the same after 1PE and 2PE (13,28), indicating that fluorescein evolves to the same excited state and thus undergoes similar excited-state dynamics after either type of excitation. We exploited these properties and used CM-H_2DCFDA and its oxidative metabolites related to DCF to act as both mediators and reporters of 2PE-directed ROS formation in fibroblasts and fibroblast-derived cells.

In near-confluent cell monolayers incubated with CM-H_2DCFDA, pulsed 800 nm irradiation of single fibroblasts resulted in a rise in intracellular fluorescence from DCF, indicating that ROS formation can be targeted to individual cells (Fig. 2). Such increased cellular fluorescence after 2PE was observed in several different cell lines, including both primary and transformed cells, indicating that the mechanism involved is not specific to a particular type of cell. There are two pieces of evidence that ROS formation in target cells results from a multiphoton excitation event and not a one-photon absorption process. First, irradiation of cells with the 800 nm output of the titanium–sapphire laser in continuous wave mode does not produce an

increase in ROS, whereas irradiation with the pulsed output of the laser using the same average power but many orders of magnitude larger peak power yields a rapid induction of ROS formation (Fig. 4). Thus, the efficiency of ROS formation with multiphoton excitation is significantly greater than with one-photon absorption at 800 nm. Second, a quadratic relationship exists between the cellular fluorescence intensity and the excitation power (Fig. 3), the hallmark of 2PE. These results unequivocally demonstrate that the observed ROS are generated as a result of 2PE and not simply 1PE at 800 nm of a weakly absorbing photosensitizer.

Our results are consistent with a model in which endogenous ROS from basal cellular metabolism generates a small amount of DCF from CM-H_2DCFDA, which then functions as a photodynamic agent to generate additional ROS after 2PE (23). ROS formation has been detected by adding H_2DCFDA immediately after broadband ultraviolet irradiation of normal human epidermal keratinocytes and observing fluorescence from DCF, suggesting the presence of endogenous photodynamic chromophores that absorb ultraviolet wavelengths (33). In contrast, incubation of cells with CM-H_2DCFDA before pulsed 800 nm irradiation resulted in significant increases in fluorescence, whereas addition of CM-H_2DCFDA immediately after 800 nm irradiation did not. Considering that short-lived singlet oxygen does not appear to react with H_2DCF (23), it seems reasonable to infer that the fluorescence observed in the presence of CM-H_2DCFDA is due to longer-lived ROS. The presence of an endogenous photosensitizer in dermal fibroblasts with a significant near-infrared 2PE cross-section is therefore unlikely, though our experiments cannot exclude that possibility.

There have been reports inferring ROS formation due to 2PE of cells both with and without exogenous photodynamic agents. Chinese hamster ovary cells treated with photofrin or amino-levulinic acid and irradiated with 780 nm pulsed laser showed decreased cloning efficiency (21). Although the absorption of photofrin is seemingly negligible at 780 nm (34), the possibility of one-photon absorption by photofrin or an endogenous chromophore giving rise to the observed effects was not considered by the authors. Pulsed 800 nm laser irradiation of rat kangaroo kidney epithelium cells, incubated with the probes of ROS formation, Ni-diaminobenzidine and Jenchrom px blue, produced ROS and led to apoptosis (19), suggesting that endogenous photodynamic chromophores are capable of multiphoton excitation. However, it is unclear in this work if the probes or their light absorbing reaction products themselves could have acted as the predominant mediators of ROS induction through either a one- or two-photon absorption event. In our experiments, if endogenous chromophores were significantly contributing to long-lived ROS induction, then adding CM-H_2DCFDA immediately after irradiation should have yielded increased fluorescence above that in unirradiated cells, which did not occur.

The generation of ROS by 2PE in two-dimensional cell culture was extended to three-dimensional dermal equivalents. These reconstituted tissue simulants have been shown to have properties that are histologically and physically similar to actual dermis (35). Individual cells within the dermal equivalent were targeted with 2PE and subsequently developed DCF fluorescence, indicative of ROS formation, whereas nearby cells within the cone of excitation light but not at the focus did not show detectable ROS formation over that in unirradiated cells (Fig. 5d,e). This capability is possible because of the quadratic dependence of ROS formation on laser intensity demonstrated in Fig. 3. This result illustrates the spatial selectivity of ROS formation in a three-dimensional biological tissue that is possible with this technique. As stated earlier, the excitation volume within which 50% of the 2PE effect is expected to occur is 0.4 μm wide and 1.5 μm above and below the focal plane, which is sufficient to target fibroblasts dispersed in dermis and even keratinocytes in epidermis. Although modest when compared with the overall dimensions of human skin, which is typically several millimeters thick, the 25 μm depth at which ROS were targeted in cells makes targeting specific keratinocytes within a

typical 50 μm murine epidermis achievable and approaches the ~ 100–200 μm thickness of human foreskin epidermis.

Targeting ROS formation to selected cells within a tissue would be useful for dissecting the damage response of highly ordered structures such as stratified epithelia where the response may vary with cellular position. In this work we demonstrate a general method for generating ROS deep inside a biomimetic tissue while sparing other cells, allowing one to ask questions about the heterogeneous organization of tissues, cell fate and communication among skin cells after genotoxic stress with a precision that is not readily available with current techniques. To our knowledge, this is the first rigorous proof of 2PE of a photodynamic agent with subsequent use of that agent to induce ROS in a biological tissue with three-dimensional specificity.

Abbreviations

CM-H_2DCFDA, 5-(and 6-)chloromethyl-2′,7′-dichlorodihydrofluorescein diacetate, acetyl ester; DCF, 2′,7′-dichlorofluorescein; DMEM, Dulbecco's modified Eagle medium; H_2DCF, 2′,7′-dichlorodihydrofluorescein; ROI, region of interest; ROS, reactive oxygen species; 2PE, two-photon excitation.

Acknowledgments

This work was supported by grants from the NIH (R01-CA105958), the UCSF Academic Senate and the VA Medical Research Service (D.H.O.) and from the Yale School of Medicine Office of Student Research (B.A.K.). We thank K. Nagayoshi for assistance with cell culture and formation of dermal equivalents, the staff of the Laboratory for Cell Analysis at the UCSF Cancer Center for technical assistance with the microscope and C. Largman for helpful comments on the manuscript.

REFERENCES

1. Sharman WM, Allen CM, van Lier JE. Role of activated oxygen species in photodynamic therapy. Methods Enzymol 2000;319:376–400. [PubMed: 10907528]
2. Gould JW, Mercurio MG, Elmets CA. Cutaneous photosensitivity diseases induced by exogenous agents. J. Am. Acad. Dermatol 1995;33:551–573. [PubMed: 7673488]
3. Kalka K, Merk H, Mukhtar H. Photodynamic therapy in dermatology. J. Am. Acad. Dermatol 2000;42:389–413. [PubMed: 10688709]
4. Anderson RR, Parrish JA. The optics of human skin. J. Invest. Dermatol 1981;77:13–19. [PubMed: 7252245]
5. Denk W, Strickler JH, Webb WW. Two-photon laser scanning fluorescence microscopy. Science 1990;24:73–76. [PubMed: 2321027]
6. Strickler JH, Webb WW. Three-dimensional optical data storage in refractive media by two-photon point excitation. Opt. Lett 1991;16:1780–1782. [PubMed: 19784138]
7. Oh DH, Stanley RJ, Lin M, Hoeffler WK, Boxer SG, Berns MW, Bauer EA. Two-photon excitation of 4′-hydroxymethyl–4,5′,8-trimethylpsoralen. Photochem. Photobiol 1997;65:91–95. [PubMed: 9066288]
8. Fisher WG, Partridge WP, Dees C, Wachter EA. Simultaneous two-photon activation of type I photodynamic therapy agents. Photochem. Photobiol 1997;66:141–155. [PubMed: 9277135]
9. Oh DH, King BA, Boxer SG, Hanawalt PC. Spatially localized generation of nucleotide sequence-specific DNA damage. Proc. Natl. Acad. Sci. USA 2001;98:11271–11275. [PubMed: 11572980]
10. Fredericksen PK, Jorgensen M, Ogilby PR. Two-photon photosensitized production of singlet oxygen. J. Am. Chem. Soc 2001;123:1215–1221. [PubMed: 11456676]
11. Poulsen TD, Fredericksen PK, Jorgensen M, Mikkelsen KV, Ogilby PR. Two-photon singlet oxygen sensitizers: quantifying, modeling, and optimizing the two-photon absorption cross section. J. Phys. Chem. A 2001;105:11488–11495.
12. Göppert-Mayer M. Elementary processes with two quantum jumps. Ann. Phys 1931;9:273–294.

13. Xu C, Webb WW. Measurement of two-photon excitation cross sections of molecular fluorophores with data from 690 to 1050 nm. J. Opt. Soc. Am. B 1996;13:481–491.
14. Lipp P, Niggli E. Fundamental calcium release events revealed by two-photon excitation photolysis of caged calcium in guinea-pig cardiac myocytes. J. Physiol 1998;508:801–809. [PubMed: 9518734]
15. Furuta T, Wang SS-H, Dantzker JL, Dore TM, Bybee WJ, Callaway EM, Denk W, Tsien RY. Brominated 7-hydroxycoumarin-4-ylmethyls: photolabile protecting groups with biologically useful cross-sections for two photon photolysis. Proc. Natl. Acad. Sci. USA 1999;96:1193–1200. [PubMed: 9990000]
16. Shafirovich V, Dourandin A, Luneva NP, Singh C, Kirigin F, Geacintov NE. Multiphoton near-infrared femtosecond laser pulse-induced DNA damage with and without the photosensitizer proflavine. Photochem. Photobiol 1999;69:265–274. [PubMed: 10232956]
17. Goyan RL, Cramb DT. Near-infrared two-photon excitation of protoporphyrin IX: photodynamics and photoproduct generation. Photochem. Photobiol 2000;72:821–827. [PubMed: 11140272]
18. Berns MW, Wang Z, Dunn A, Wallace V, Venugopalan V. Gene inactivation by multiphoton-targeted photochemistry. Proc. Natl. Acad. Sci. USA 2000;97:9504–9507. [PubMed: 10944219]
19. Tirlapur UK, König K, Peuckert C, Krieg R, Halbhuber KJ. Femtosecond near-infrared laser pulses elicit generation of reactive oxygen species in mammalian cells leading to apoptosis-like death. Exp. Cell. Res 2001;263:88–97. [PubMed: 11161708]
20. Dees C, Harkins J, Petersen MG, Fisher WG, Wachter EA. Treatment of murine cutaneous melanoma with near infrared light. Photochem. Photobiol 2002;75:296–301. [PubMed: 11950096]
21. König K. Multiphoton microscopy in life sciences. J. Microsc 2000;200:83–104. [PubMed: 11106949]
22. Marchesi E, Rota C, Fann YC, Chignell CF, Mason RP. Photoreduction of the fluorescent dye 2′-7′-dichlorofluorescein: a spin trapping and direct electron spin resonance study with implications for oxidative stress measurements. Free Radic. Biol. Med 1999;26:148–161. [PubMed: 9890650]
23. Bilski P, Belanger AG, Chignell CF. Photosensitized oxidation of 2′,7′-dichlorofluorescin: singlet oxygen does not contribute to the formation of fluorescent oxidation product 2′,7′-dichlorofluorescein. Free Radic. Biol. Med 2002;33:938–946. [PubMed: 12361804]
24. Chignell CF, Sik RH. A photochemical study of sells loaded with 2′,7′-dichlorofluorescin: implications for the detection of reactive oxygen species generated during UVA irradiation. Free Radic. Biol. Med 2003;34:1029–1034. [PubMed: 12684087]
25. Lin M, Hultquist K, Oh DH, Hoeffler WK, Bauer EA. Inhibition of collagenase type I expression by psoralen-antisense oligonucleotides in dermal fibroblasts. FASEB J 1995;9:1371–1377. [PubMed: 7557028]
26. Oh DH, Hanawalt PC. Triple helix-forming oligonucleotides target psoralen adducts to specific chromosomal sequences in human cells. Nucleic Acids Res 1999;27:4734–4742. [PubMed: 10572173]
27. Haugland, RP. Handbook of Fluorescent Probes and Research Products. Eugene, OR: Molecular Probes; 2002. p. 756
28. Xu C, Zipfel W, Shear JB, Williams RM, Webb WW. Multiphoton fluorescence excitation: new spectral windows for biological nonlinear microscopy. Proc. Natl. Acad. Sci. USA 1996;93:10763–10768. [PubMed: 8855254]
29. Wirth MJ, Fatunmbi HO. Very high detectability in two-photon spectroscopy. Anal. Chem 1990;62:973–978.
30. Meldrum RA, Botchway SW, Wharton CW, Hirst GJ. Nanoscale spatial induction of ultraviolet photoproducts in cellular DNA by three-photon near-infrared absorption. EMBO Rep 2003;4:1144–1149. [PubMed: 14618160]
31. Cahalan M, Parker I, Wei S, Miller M. Two-photon tissue imaging: seeing the immune system in a fresh light. Nat. Rev. Immunol 2002;2:872–880. [PubMed: 12415310]
32. Stosiek C, Garaschuk O, Holthoff K, Konnerth A. In vivo two-photon calcium imaging of neuronal networks. Proc. Natl. Acad. Sci. USA 2003;100:7319–7324. [PubMed: 12777621]
33. Pelle E, Huang X, Mammone T, Marenus K, Maes D, Frenkel K. Ultraviolet-B-induced oxidative DNA base damage in primary normal human epidermal keratinocytes and inhibition by a hydroxyl radical scavenger. J. Invest. Dermatol 2003;121:177–183. [PubMed: 12839579]

34. Bonnett, R. Chemical Aspects of Photodynamic Therapy. Amsterdam: Gordon and Breach Science Publishers; 2000.

35. Bell E, Sher S, Hull B, Merrill C, Rosen S, Chamson A, Asselineau D, Dubertret L, Coulomb B, Lapiere C, Nusgens B, Neveux Y. The reconstitution of living skin. J. Invest. Dermatol 1983;81:2s–10s. [PubMed: 6306115]

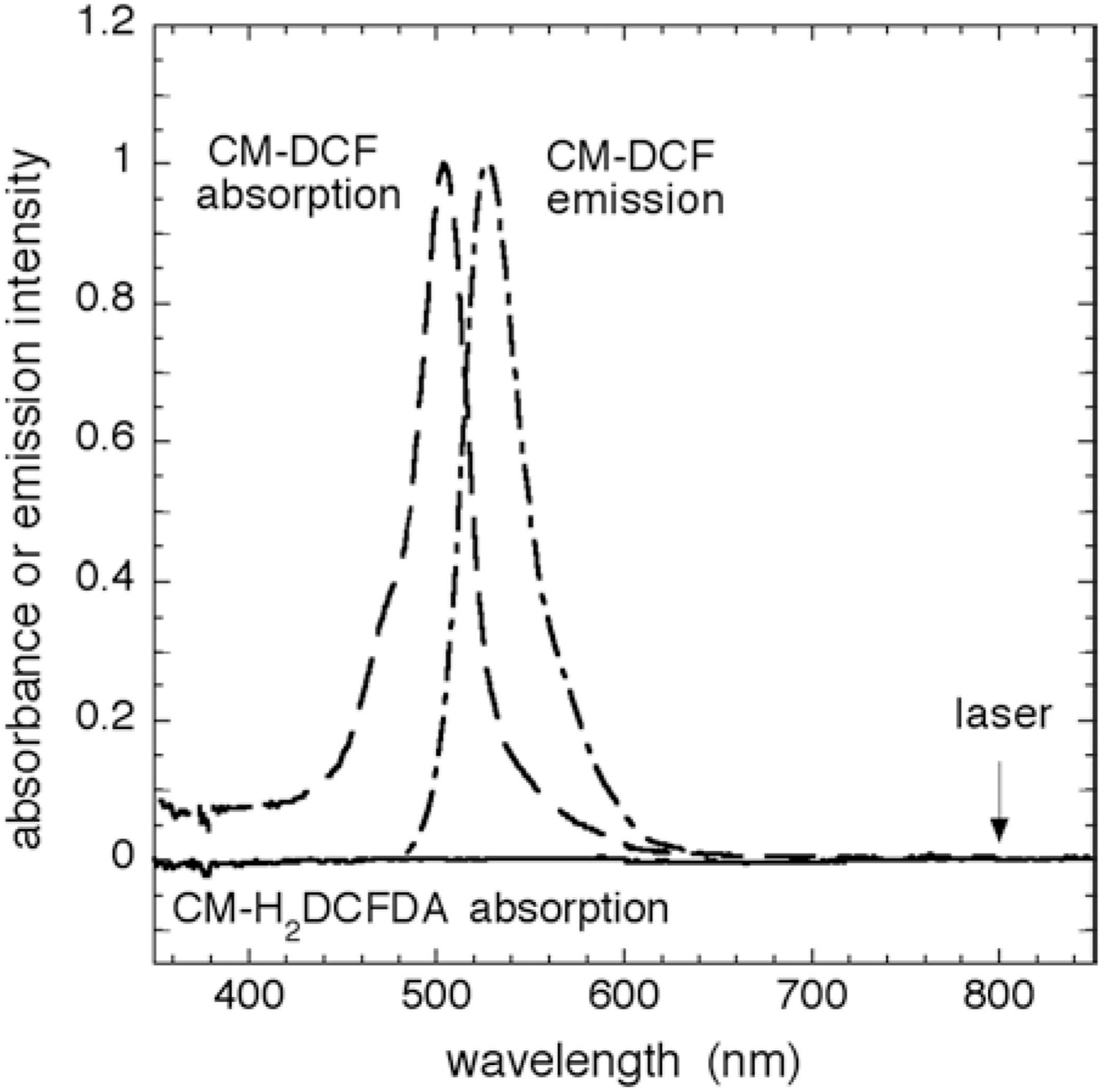

Figure 1.

Spectra of CM-H_2DCFDA and its oxidation products. Absorption spectra of CM-H_2DCFDA (10 μ*M*) in PBS, pH 7.4 (——), and 2 h after addition of 100 μ*M* H_2O_2 to generate CM-DCF (— —). HT1080 cells were incubated with 10 μ*M* CM-H_2DCFDA at 37°C for 30 min followed by treatment with 100 μ*M* H_2O_2 for 10 min to generate the DCF moiety intracellularly. The peak of the resulting uncorrected single-cell fluorescence spectrum (–·–·–·–) is normalized to the absorption maximum. The arrow indicates the output wavelength of the titanium–sapphire laser.

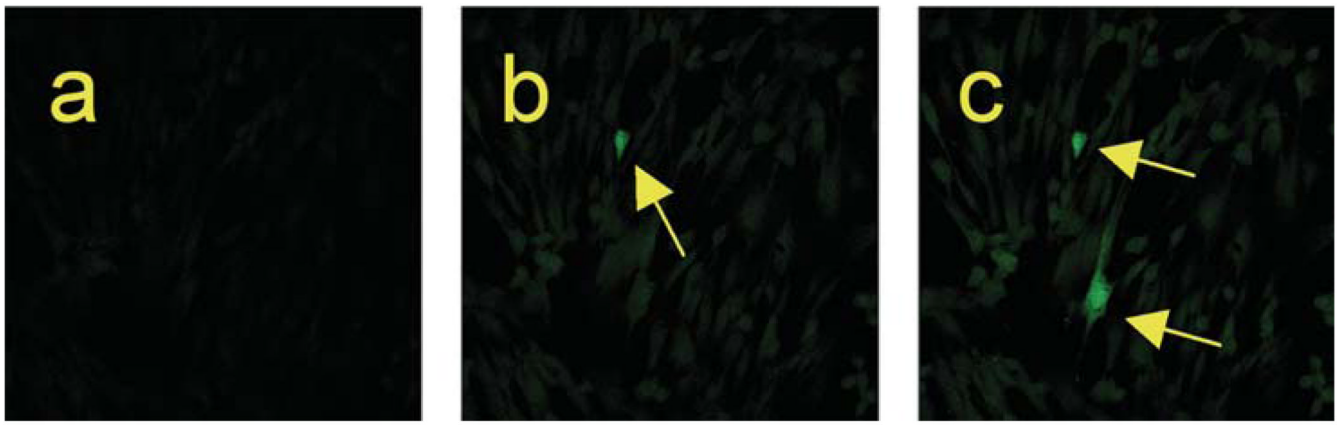

Figure 2.

Intracellular generation of ROS by pulsed 800 nm irradiation. Normal human dermal fibroblasts grown as a monolayer on borosilicate slides were incubated with 4 μ*M* CM-H_2DCFDA. The field was observed with 488 nm excitation (a) before 2PE, (b) after 2PE to a single cell in the upper half of the field for 3 min, and (c) after 2PE to a single cell in the lower half of the field for 6 min. 2PE was performed by irradiating an oval region of interest approximately corresponding to the interior of the cell body with 12 mW of pulsed 800 nm light with a pixel dwell time of 25 μs.

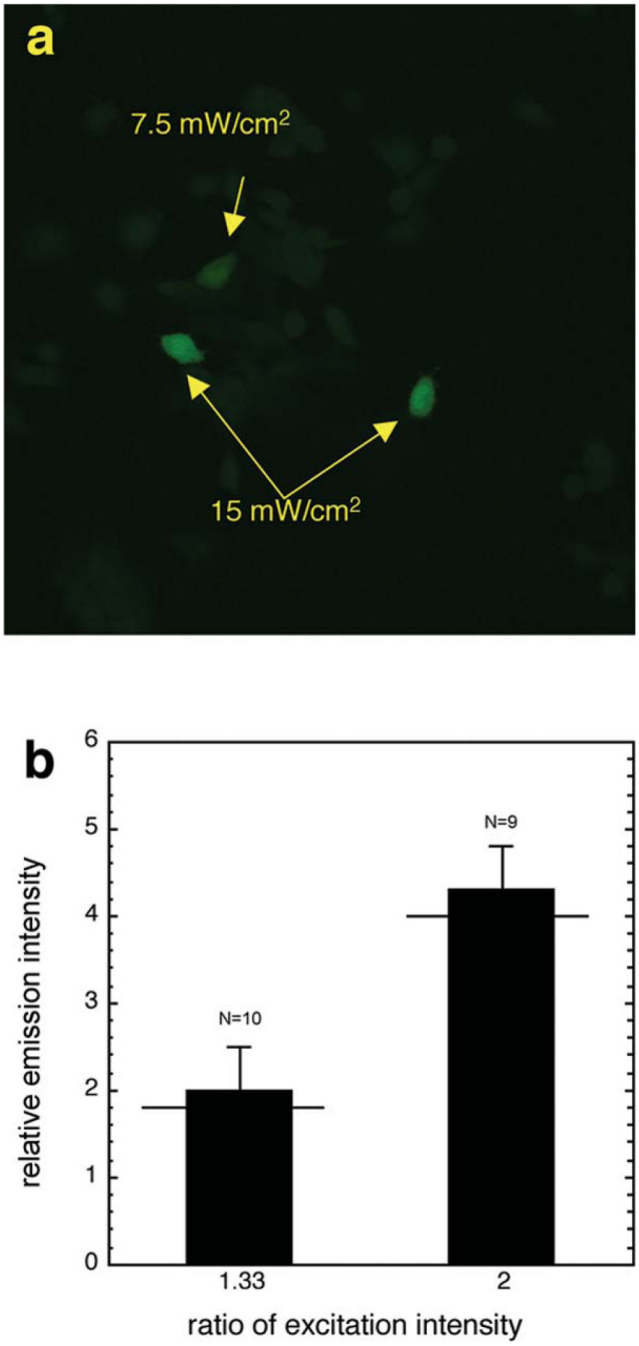

Figure 3.

Quadratic dependence of ROS formation on excitation power. (a) XP12RO-SV40 cells grown as a monolayer on borosilicate slides were incubated with 10 μ*M* CM-H_2DCFDA, and selected cells of similar size were then irradiated with either 7.5 or 15 mW of 800 nm pulsed titanium–sapphire laser and observed. (b) Comparison of cellular fluorescence intensities for different excitation powers. Pairs of cells were irradiated, with one of the two cells getting either 1.33 or 2 times the excitation power applied to the other cell. The fluorescence intensity of each cell was then measured and the ratio of intensity calculated for each pair of cells. N = the number of pairs of cells irradiated. The horizontal lines mark the predicted values of relative fluorescence intensity for 2PE. The maximum excitation power was 18 mW.

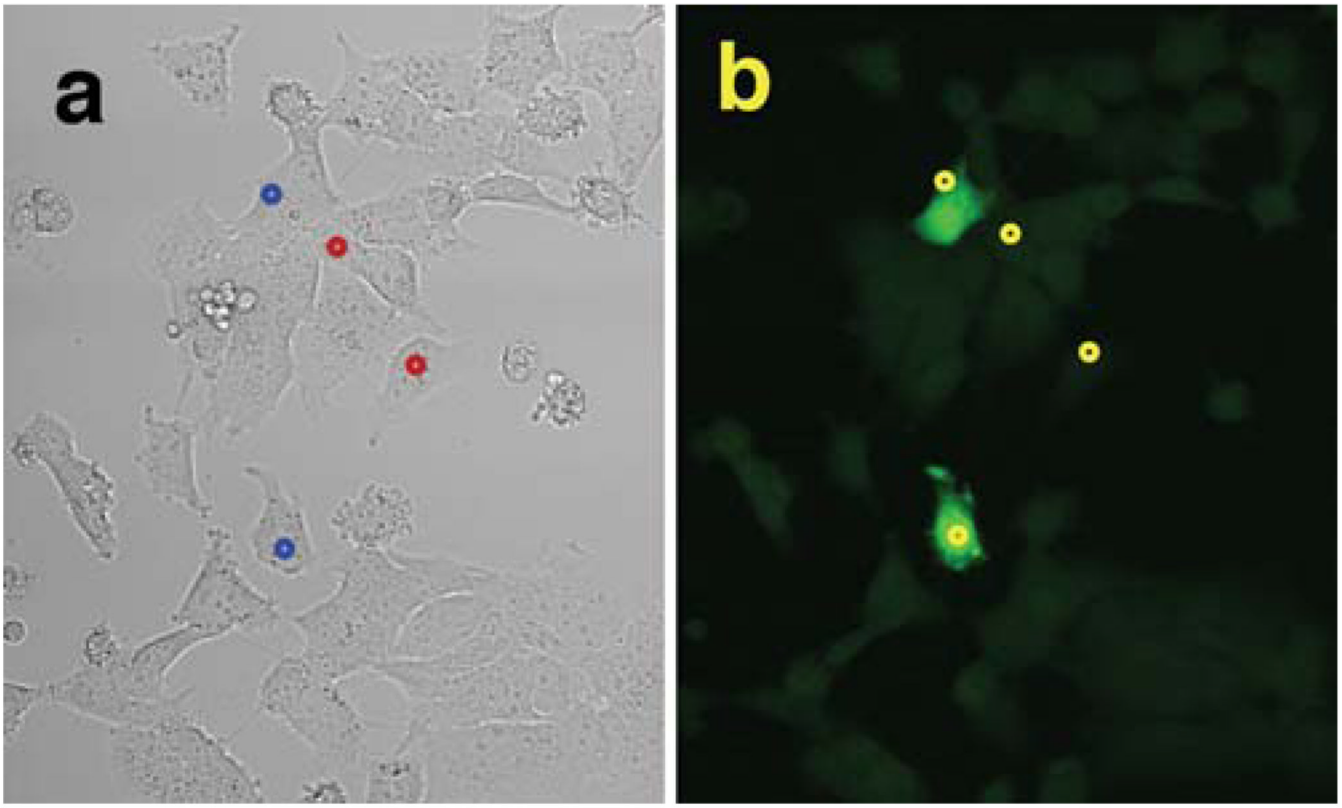

Figure 4.
One- *versus* two-photon excitation. XP12RO-SV40 cells grown as a monolayer on borosilicate slides were incubated with 10 μ*M* CM-H_2DCFDA. (a) Transmission of the 633 nm line of the helium–neon laser through the monolayer permitted observation of the cells. The circles depict the regions of cells that were irradiated with either continuous wave (red circles) or pulsed (blue circles) 800 nm titanium–sapphire laser at an average power of 15 mW. (b) Observation of cells after irradiation as described above.

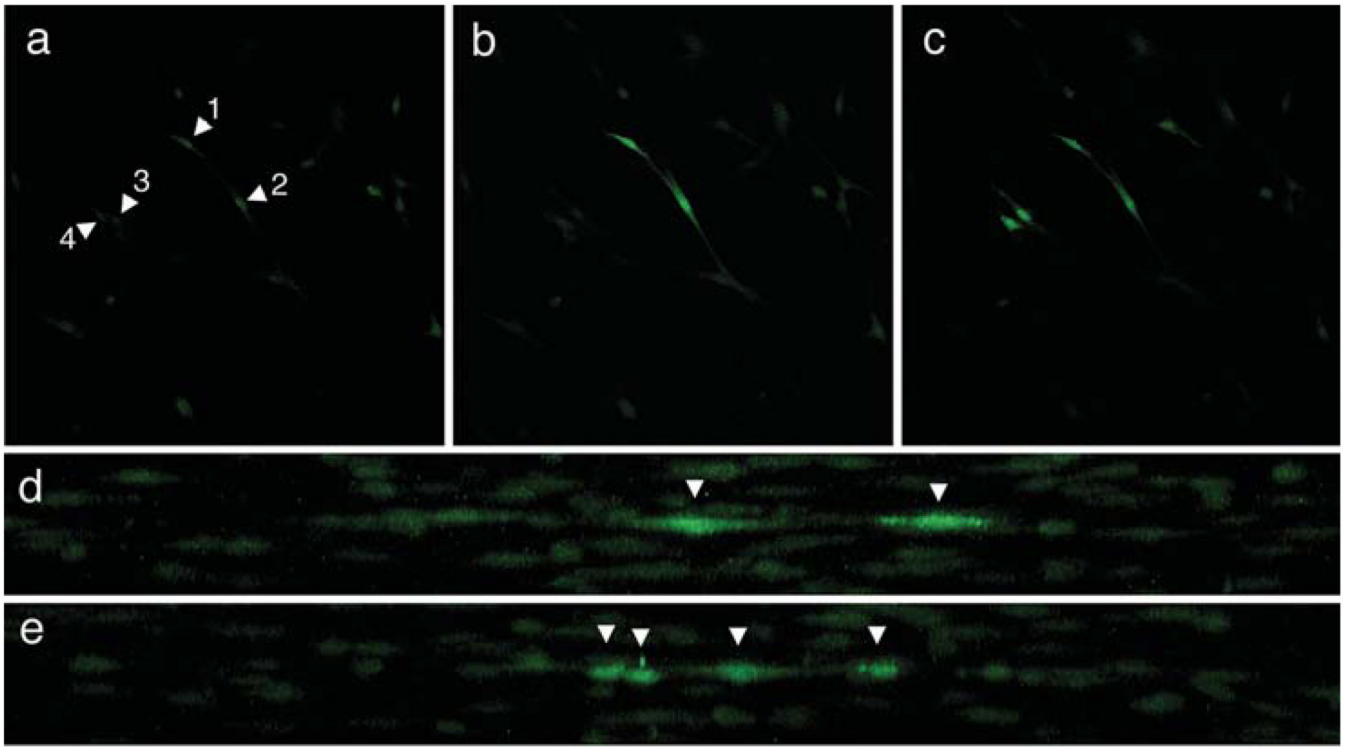

Figure 5.
Targeted formation of ROS in a dermal equivalent. Fibroblasts within a collagen matrix were incubated with 10 μ*M* CM-H_2DCFDA. (a) Fibroblasts in a plane 25 μm deep inside the dermal equivalent before irradiation with the 800 nm pulsed titanium–sapphire laser. Arrowheads indicate target cells. (b) 25 μm plane after irradiation of the two cells labeled 1 and 2 in panel a. (c) 25 μm plane after irradiation of two additional cells labeled 3 and 4 in panel a. (d) Projection image of cells in all planes from 0 to 50 μm deep in the dermal equivalent after irradiation of the two cells shown in panel (b). Cells from all planes have been projected onto a plane perpendicular to the dermal equivalent. Arrowheads indicate the two target cells. (e) Projection image of cells in all planes from 0 to 50 μm deep in the dermal equivalent after irradiation of two additional cells shown in panel (c). Cells from all planes have been projected onto a plane perpendicular to the dermal equivalent. Note that the projection direction differs from panel (d) to demonstrate all four target cells optimally. Arrowheads indicate the four cells.